Variability of seasonal and annual rainfall in the River Nile riparian countries and possible linkages to ocean–atmosphere interactions

Charles Onyutha

Charles Onyutha
Faculty of Technoscience,
Muni University,
P.O. Box 725,
Arua,
Uganda
E-mail: conyutha@gmail.com

ABSTRACT

Variability analyses for the rainfall over the Nile Basin have been confined mostly to sub-basins and the annual mean of the hydroclimatic variable based on observed short-term data from a few meteorological stations. In this paper, long-term country-wide rainfall over the period 1901–2011 was used to assess variability in the seasonal and annual rainfall volumes in all the River Nile countries in Africa. Temporal variability was determined through temporal aggregation of series rescaled nonparametrically in terms of the difference between the exceedance and non-exceedance counts of data points such that the long-term average (taken as the reference) was zero. The co-occurrence of the variability of rainfall with those of the large-scale ocean–atmosphere interactions was analyzed. Between 2000 and 2012, while the rainfall in the equatorial region was increasing, that for the countries in the northern part of the River Nile was below the reference. Generally, the variability in the rainfall of the countries in the equatorial (northern) part of the River Nile was found to be significantly linked to occurrences in the Indian and Atlantic (Pacific and Atlantic) Oceans. Significant linkages to Niño 4 regarding the variability of both the seasonal and annual rainfall of some countries were also evident.

Key words | climate indices, climate variability, nonparametric anomaly indicator method, ocean–atmosphere interactions, rainfall variability, River Nile

INTRODUCTION

The River Nile is the world's longest river under arid conditions and is fed by two main river systems: the White Nile (from the equatorial region) and the Blue Nile (from the Ethiopian highlands) (Onyutha & Willems 2015a). The river has a basin with a total catchment area of about 3,400,000 km² stretching over 35° of latitude in the north–south direction (31 °N to 4 °S) and over 16° of longitude in the west–east direction (24 °E to 40 °E) (Onyutha & Willems 2015a). The River Nile riparian countries include Burundi, Rwanda, Uganda, Kenya, Tanzania, South Sudan, Democratic Republic of Congo (DRC) (formerly known as Zaire), Sudan, Eritrea, Ethiopia, and Egypt (see Figure 1). The climate of the River Nile countries is characterized by a strong latitudinal wetness gradient. Whereas some parts experience hyper-aridity, substantial areas exhibit sub-humid conditions (Onyutha & Willems 2015a). Annual rainfall in excess of 1,000 mm is restricted mainly to the equatorial region and the Ethiopian highlands (Camberlin 2009). From the northern Sudan all across Egypt, rainfall is negligible (below 50 mm except along the Mediterranean coast). This general distribution reflects the latitudinal movement of the inter-tropical convergence zone (ITCZ) which never reaches Egypt and the northernmost part of Sudan, staying only briefly in central Sudan and longer further south (Camberlin 2009).

The weather system's variability is a crucial issue in water and agricultural management especially in the tropics and its stationarity for any extended period is highly unlikely. According to the International Water Management Institute
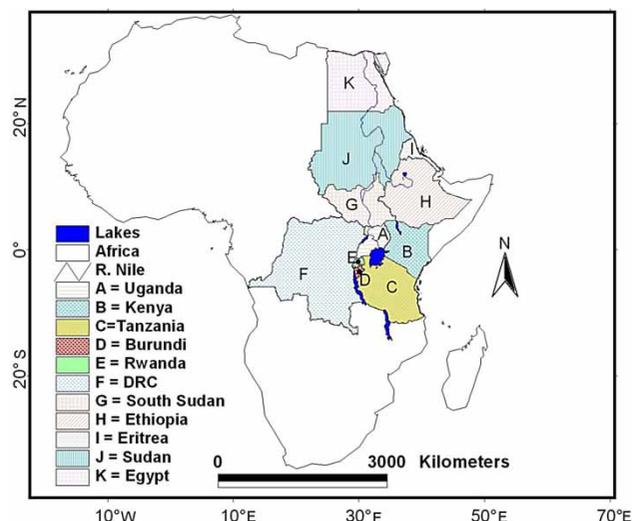
Figure 1 | River Nile riparian countries (see Table 1 for area coverage).

(IWMI) (2014), over 70% of the people within the Nile Basin depend on subsistence rain-fed agriculture for their livelihoods. This situation is becoming more problematic with increasingly unpredictable rainfall (IWMI 2014). According to Melesse et al. (2011), subsistence and rain-fed agriculture, together with high rainfall variability, is one of the main causes of food insecurity and the most daunting challenge the basin faces. Unpredictability of the rainfall is reflected in terms of the low crop yields, unsustainable water use, etc. Due to the variability in the rainfall, river flows in the

Nile Basin will be affected (Melesse et al. 2011). This will lower the reliability of the water available for irrigation, hydropower, etc. in the basin (McCartney & Girma 2012).

The climate variability, through its influences on the occurrences of rainfall extremes, has also greatly shaped the frequency, severity, and locations of floods and droughts in the Nile Basin. In the history of flooding in the Nile Basin, Ethiopia, Tanzania, Kenya, Sudan, and Uganda are the most affected countries in terms of the average number of flooding occurrences (Kibiiy et al. 2010). Heavy rainfall events over Khartoum and Atbara led to severe flooding in Sudan during August–September 1988 (Sutcliffe et al. 1989). The prolonged drought in the Greater Horn of Africa that ended in 2005 was followed by severe flooding in August 2006 (Nawaz et al. 2010). In the Lake Victoria Basin, despite the frequent episodes of floods in the low-lying parts (Gichere et al. 2013), in other areas long periods of drought can occur.

Apart from the questionable data quality, the accuracy in the estimation of quantiles in support of water management applications in the study area is also influenced by climate variability. For data of limited record length, Taye & Willems (2011) showed that the values of the extreme events or quantiles can be biased from those of the long term due to the decadal or multi-decadal climate oscillations. For the hydrometeorological quantiles of the Nile Basin, this has prompted both at-site uncertainty

Table 1 | Overview of River Nile countries and their annual rainfall data

| S no. | Country | Area (km²) | | Area (%) | | Rainfall (mm/year) | | | | |
		TAC	ACWB	PTAB	PTAC	MAX	S_D	C_v	C_s	K_u
1	Uganda	235,880	231,366	7.40	98.10	1560.8	114.14	0.10	0.14	1.13
2	Kenya	580,370	46,229	1.50	8.00	1067.4	120.88	0.19	0.91	1.56
3	Tanzania	945,090	84,200	2.70	8.90	1327.5	122.82	0.12	0.38	−0.22
4	Rwanda	26,340	19,876	0.60	75.50	1471.6	138.11	0.12	0.02	0.03
5	Burundi	27,834	13,260	0.40	47.60	1533.9	137.83	0.12	0.12	0.23
6	DRC	2,344,860	22,143	0.70	0.90	1755.3	69.19	0.05	−0.29	2.31
7	Sudan	2,505,810	1,978,506	63.60	79.00	540.5	46.81	0.11	−0.53	1.07
8	Ethiopia	1,100,010	365,117	11.70	33.20	1165.6	95.44	0.11	0.59	0.70
9	Eritrea	121,890	24,921	0.80	20.40	649.3	75.40	0.20	1.01	1.50
10	Egypt	1,001,450	326,751	10.50	32.60	67.3	9.76	0.23	0.36	−0.42

TAC, total area of the country; ACWB, area of the country within the Nile basin; PTAB, as a percentage of total area of Nile basin; PTAC, as a percentage of area of the country; MAX, long-term maximum event; S_D, standard deviation; C_v, coefficient of variation; C_s, skewness; K_u, actual excess kurtosis.

quantification (Kizza et al. 2011; Onyutha & Willems 2013, 2015b) and regionalization procedures (Nyeko-Ogiramoi et al. 2012; Kizza et al. 2013; Onyutha & Willems 2015c). However, the data used in the above studies on the at-site and regional analyses are based on only a few hydrometeorological stations and are of short record lengths.

Understanding variability in rainfall is a critical factor, among other meteorological variables to determine the influence of the climate system on hydrology in support of risk-based water resources management. Possible driving forces of rainfall variability might come from the large scale ocean–atmosphere interactions and/or anthropogenic factors. Assessment of the co-occurrence of the rainfall variability with those of the large ocean–atmosphere interactions can be valuable especially in predicting the upcoming periods of decrease or increase in rainfall for sustainable use and management of water resources. Some of the studies undertaken on rainfall variability in the study area include Ogallo (1989), Semazzi & Indeje (1999), Indeje et al. (2000), Mbungu et al. (2012), Taye & Willems (2012), Nyeko-Ogiramoi et al. (2013), Moges et al. (2014), and Onyutha & Willems (2015a). In some of these studies, the variability analyses were confined mostly to sub-basins and annual mean of the rainfall and, moreover, based on observed short-term data selected over different time periods and from a few meteorological stations. These could altogether affect the spatial coherence of results for the variability analyses. Instead of just annual rainfall, variability in the seasonal volumes is also important for the basin given its dependency on the rain-fed irrigation system. In some of the above studies, e.g., Mbungu et al. (2012), there were no attempts to investigate any possible linkages of the rainfall variability to ocean–atmosphere interactions. In the methods used to analyze variability in the above (cited) studies, rainfall intensity values were applied directly. In such cases, computed variability anomalies may be exaggerated if there are possible outliers in the data. An option would be to use ranks of the data values for the variability analysis as tested in this study. Therefore, this study was aimed at assessing the rainfall variability of both seasonal and annual volumes in all the River Nile countries while exploring any possible linkages to the ocean–atmosphere interactions. This was done while considering the following: the country-wide long-term rainfall data over the same time period; computation of variability anomalies in a non-parametric way; and using a number of climate indices relevant to explaining the variability in the rainfall over the River Nile Basin.

When it comes to the computation of rainfall variability, different methods exist. The key ones are empirical orthogonal functions and autocorrelation spectral analysis. The empirical orthogonal function applies principal component analysis to a group of rainfall time series data to extract coherent variations that are dominant. It entails the computation of eigenvectors and eigenvalues of a covariance or a correlation matrix obtained from a group of original rainfall time series data. This method was applied on rainfall variability in the Nile Basin by, for example, Ogallo (1989), Semazzi & Indeje (1999), and Indeje et al. (2000). However, the analysis of empirical orthogonal functions can be sensitive to the choice of spatial domain and the time period. It is also possible that empirical orthogonal function analysis can create patterns from 'noise'. Physical interpretation of such patterns from 'noise' becomes complicated and unreliable. According to Bretherton et al. (1992), although the method of empirical orthogonal functions is satisfactory over a wide range of data structures, it is certainly not universally optimal. The autocorrelation spectral analysis (Blackman & Tukey 1959; World Meteorological Organization (WMO) 1966) utilizes the connection of autocovariance estimation and spectral analysis by the Fourier transform. This method was applied by Nicholson & Entekhabi (1986) to assess the quasi-periodic behavior of rainfall variability in Africa and its relationship to Southern Oscillation. Recently, Ntegeka & Willems (2008) used a quantile perturbation method to study variability in rainfall extremes at Uccle in Belgium. The quantile perturbation method compares two series to obtain relative perturbation factors that are used to represent the variability. One of the series is taken to be the full time data set, while the other is a block of sample points picked from the entire historical period. This method was applied in a number of studies of the Nile Basin; see Taye & Willems (2012) and Moges et al. (2014) for the Blue Nile Basin, and Mbungu et al. (2012) and Nyeko-Ogiramoi et al. (2013) for Lake Victoria Basin. However, the quantile perturbation method is applicable to quantitative series, and for qualitative data sets such as temperature, Nyeko-Ogiramoi et al. (2013) proposed absolute

values to be adopted through conversion from degree Celsius (°C) to Kelvin (K). This conversion from °C to K is a standard procedure to make values of the entire data positive. There are, however, other series with both negative and positive values, e.g., the Atlantic Multidecadal Oscillation (AMO) index, the Southern Oscillation Index (SOI), etc., as used in this study which do not have any standard procedure of conversion to only positive values without losing relevant statistics from the original data. Applying the quantile perturbation method to such series directly may, therefore, yield unrealistic perturbation factors over some time slices. In this study, temporal variability is examined by an approach herein referred to as the nonparametric anomaly indicator method (NAIM). It is mainly based on the rescaling of series nonparametrically in terms of the difference between the exceedance and non-exceedance counts of data points such that the long-term average (taken as the reference) is zero (Onyutha 2016). The use of ranks during the rescaling of series ensures that the NAIM is not affected by non-normally distributed data which frequently occur in hydrometeorology.

DATA

Rainfall

Country-wide monthly series of rainfall over the River Nile countries for the period 1901–2011 were obtained via the British Atmospheric Data Centre (BADC) (2014). The said series were from the Climatic Research Unit (CRU) year-by-year variation of selected climate variables by CountrY (CY) available as CRU CY 3.21 data (Harris *et al.* 2014). For the procedural details of how the CRU CY 3.21 data were processed and obtained, the reader is referred to BADC (2014). Important to note is that the CRU CY 3.21 data sets prioritized completeness, and had no missing data (BADC 2014). Through pre-analysis checks, the obtained rainfall data for the River Nile countries before their use in this study were confirmed to have no missing data. Although South Sudan became independent from Sudan in 2011, the CRU CY 3.21 data set under the name Sudan comprises averages over the two countries.

From the monthly series, seasonal and annual rainfall totals were obtained for analyses of the temporal variability. Variability of rainfall volumes as considered in this study is important for management of agricultural practices. Table 1 shows for all the countries the data record length, long-term maximum total (MAX), standard deviation (S_D), coefficient of variation (C_v), skewness (C_s), and actual excess kurtosis (K_u) of the annual rainfall time series. Since for a normal distribution it is expected that $C_s = 0$ and $K_u = 0$, it can be said that the rainfall data for the different countries were, on average, slightly positively skewed ($C_s = 0.272$) and marginally leptokurtic ($K_u = 0.787$). Compared with the normal distribution, the central peak of the leptokurtic distribution is higher and sharper, and its tails are longer and fatter. However, the highest absolute values of C_s and K_u for the annual rainfall were 1.01 and 2.31 in Eritrea and DRC, respectively. With respect to the annual rainfall, the C_v ranged from 0.05 (DRC) to 0.23 (Egypt), which showed a moderate variability on a year-to-year basis in the study area. Generally, the latitudinal decrease in the rainfall statistics from upstream to downstream of the River Nile is also reflected in the higher magnitude of the runoff values and its variability in the southern rather than the northern part (Nyeko-Ogiramoi *et al.* 2012). Ethiopia, Sudan, Eritrea, and Egypt, i.e., countries in the northern half of the River Nile, showed lower values of S_D than those of the equatorial region (Uganda, Kenya, Tanzania, Rwanda, Burundi, and DRC). The information presented in columns 2 to 5 of Table 1 was obtained online from Food and Agriculture Organization (FAO) via the link http://www.fao.org/ (last accessed on 18 July 2014).

Series related to the large ocean–atmosphere interactions

An increase or decrease in the sea level atmospheric pressure, i.e., the sea level pressure, can reveal useful information on the atmospheric circulation which brings about the drier and wetter conditions, respectively (Onyutha & Willems 2015a). Changes in the sea surface temperature (SST), on the other hand, can generate an imbalance in the heat-flux field which can also bring about the anomalous atmospheric circulation and rainfall patterns (Horel 1982). To gain an insight into the consequences of rainfall variability due to the

pressure changes occurring in different oceans and the anomaly in circulation due to the SST (Onyutha & Willems 2015a), the following readily and freely available climate indices were used:

(1) The SOI is defined as the normalized pressure difference between Tahiti and Darwin. The SOI data based on Ropelewski & Jones (1987) were obtained from the CRU (see Table 2).

(2) The AMO index is defined as the SST averaged over $25°–60°N$, $7°–70°W$ minus the regression of this SST on global mean temperature (van Oldenborgh et al. 2009). Although Trenberth & Shea (2006) included the tropical region in their definition of the AMO, van Oldenborgh et al. (2009) decided to leave it out since it is also influenced by the El-Niño Southern Oscillation (ENSO). The AMO index was obtained from the Koninklijk Nederlands Meteorologisch Instituut through their climate explorer.

(3) The Pacific Decadal Oscillation (PDO) index is the leading principal component of the North Pacific monthly SST variability (poleward of $20°N$ in the Pacific Basin). The digital values of the PDO index of Mantua et al. (1997) were obtained from the database of the Joint Institute for the Study of the Atmosphere and Ocean.

(4) The Indian Ocean Dipole (IOD) is the anomalous SST difference between the western ($50°E$ to $70°E$ and $10°S$ to $10°N$) and the south-eastern ($90°E$ to $110°E$

and $10°S$ to $0°N$) equatorial Indian Ocean. The IOD series was obtained from the Japan Agency for Marine-Earth Science and Technology.

(5) The area averaged Niño SST indices (Trenberth 1997; Rayner et al. 2003) for the tropical Pacific region described by Niño 4 ($150°W$ to $160°E$ and $5°N$ to $5°S$) were obtained from the Earth System Research Laboratory of the National Oceanic and Atmospheric Administration.

The above climate indices were considered for this study because they were found to be relevant in explaining the variability patterns of rainfall over the Nile Basin in a number of studies including those of Taye & Willems (2012), Nyeko-Ogiramoi et al. (2013), Moges et al. (2014), and Onyutha & Willems (2015a).

METHODOLOGY

Spatial differences in rainfall statistics

Differences across the study area were assessed in terms of dry and wet seasons. This was done using the long-term mean of the monthly rainfall in the different countries. Differences in the annual rainfall totals were also examined. Strong spatial differences of these rainfall statistics could indicate differences in possible driving forces of the temporal variability in the River Nile countries.

Detection of variability using the NAIM

To assess homogeneity, variability, persistence, non-stationarity, shift in the record mean, etc. in rainfall, rescaling of the data is important. One way to do this is by applying the parametric approach in which the deviation of each data point from the mean is accumulated into partial sums and divided by the standard deviation (see, e.g., Hurst 1951; Buishand 1982). Parametric rescaling can be sensitive to possible outliers in the series. Without the need to directly use the mean and standard deviation for rescaling, and to circumvent the possible influence due to outliers in the series, a nonparametric approach is to compute the difference (D) between the exceedance and non-exceedance

Table 2 | List of series related to the ocean–atmosphere interactions

Data	Downloaded from:	Accessed on:	Period
SOI	http://www.cru.uea.ac.uk/cru/data/soi/	29 January 2013	1900–2004
AMO	http://climexp.knmi.nl/data/iamo_hadsst2.dat	29 January 2013	1900–2012
PDO	http://jisao.washington.edu/pdo/PDO.latest	30 January 2013	1900–2011
IOD	http://www.jamstec.go.jp/frcgc/research/d1/iod	20 January 2014	1900–2003
Niño 4	http://www.esrl.noaa.gov/psd/gcos_wgsp/Timeseries/Nino4/	29 January 2013	1900–2012

SOI, Southern Oscillation Index; PDO, Pacific Decadal Oscillation index; AMO, Atlantic Multidecadal Oscillation; IOD, Indian Ocean Dipole.

counts for sample points (Onyutha 2016). To do so while maintaining the fluctuation or randomness pattern in the original series, D can be given by:

$$D(i) = R_b(i) - R_a(i) \quad for\ 1 \leq i \leq n \tag{1}$$

where R_b is the number of times a data point exceeds others and R_a is the number of times a data point is exceeded. To determine R_b and R_a, each data point is counted as if it had not been considered before. For illustration, consider the hypothetical series 22, 11, 22, 19, 10; the values of R_b (R_a) are 3, 1, 3, 2, 0 (0, 3, 0, 2, 4). Correspondingly, the values of D for the given series are 3, −2, 3, 0, −4. Further application of this nonparametric rescaling in terms of negative D, i.e., ($R_a − R_b$) for both graphical and statistical detection of linear trend and sub-trends in hydro-meteorological series can be obtained from Onyutha (2016).

This nonparametric rescaling (Equation (1)) ensured the original series remained unchanged except for its mean which became zero. This was vital to separate the clusters of rainfall which could appear either below or above the long-term average. The next step was to smoothen the fluctuations in the given rainfall series by passing a moving averaging window of a particular duration (block length L_b) through the full time series.

Therefore, to determine the variability in the given series using the NAIM, the steps included:

(1) selecting the L_b;
(2) rescaling of the series using Equation (1);
(3) performing an overlapping temporal aggregation to obtain the mean (M_v) of the rescaled series $D(i)$ of Step (2) in each slice j using

$$M_v(j) = \frac{1}{L_b} \sum_{i=j}^{i=ww} D(i) \tag{2}$$

where $ww = j + (L_b−1)$ and $1 \leq j \leq (n + 1 − L_b)$;

(4) obtaining the absolute maximum value (AMV) from the aggregated series $M_v(j)$ of Step (3);
(5) calculating anomaly, expressed in terms of percentage, as a ratio of the $M_v(j)$ to AMV; and
(6) plotting the anomaly (%) against the mid-points of the time slices.

The time step of the L_b in this study was taken as one year. In Step (6), the average conditions over the long term were represented by zero percent, and the values of the changes below and above were expected to characterize the temporal variation.

To assess the sensitivity of the block length L_b (i.e., a subseries of the full time data set covering the period of interest), preliminary analysis was conducted using block periods of 5, 10, and 15 years. The choice of L_b is subjective and may depend on the objective of the study. The value of $L_b = 10$ years was found to give a much clearer anomaly pattern in the rainfall data than for 5 and 15 years, and was eventually adopted for this study.

To understand variability in rainfall and/or the driving forces, the NAIM was applied to:

(1) series of annual rainfall totals and mean of climate indices in each year; and
(2) series of seasonal rainfall totals and mean of climate indices in the corresponding season.

Test of significance in the NAIM

The null hypothesis (H_0) that the observed variability in the rainfall is caused by only the natural randomness (i.e., there is no persistence in the temporal climate variation) was considered. To verify the said hypothesis at a given level of significance (α%), nonparametric bootstrapping (Davidson & Hinkley 1997) by Monte Carlo simulations was employed. Consider N_{MC} as the number of Monte Carlo simulations; the bounds of variability using (100–α)% confidence interval (CI) were established as follows:

(1) anomaly values were obtained in the original series by applying the NAIM;
(2) the original full time series was randomly shuffled to obtain a new temporal sequence;
(3) the new series was divided to obtain subseries each of length equal to the block length L_b;
(4) the NAIM was applied to the shuffled series to obtain new temporal variation of anomalies;
(5) Steps (2)–(4) were repeated N_{MC} times to obtain N_{MC} anomaly values for each subseries;
(6) the anomaly values were ranked from the highest to the lowest; and

(7) the upper (UL) and lower (LL) limits of the $(100-\alpha)\%$ confidence interval (CI) were taken as the $[0.005 \times \alpha \% \times N_{MC}]^{th}$ and $[\{1-(0.005 \times \alpha\%)\} \times N_{MC}]^{th}$ anomaly values, respectively.

If the anomaly values from Step (1) fell within the CI, H_0 (natural randomness) was accepted; otherwise rejected. For the rejection, the UL or LL limit of CI from Step (7) was, respectively, required to be up- or down-crossed by the anomaly values. The values of N_{MC} and $\alpha\%$ were set to 1,000 and 5%, respectively.

Figure 2 shows an example of the temporal pattern of anomaly in the rainfall of March to May (MAM) season in
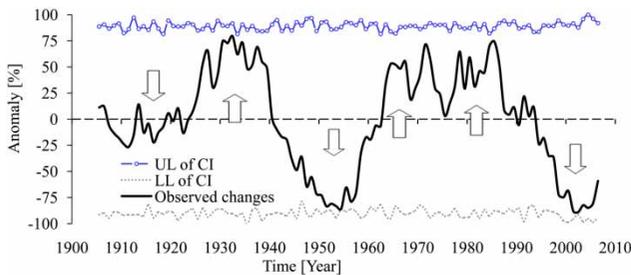
Figure 2 │ Results from the NAIM applied to the March to May (MAM) rainfall using a time slice of 10 years over the period 1901–2011; UL (LL) is the upper (lower) limit of the 95% confidence interval (CI).

the DRC. The up and down arrows indicate periods with rainfall above and below the reference, respectively. Since the 95% CI limits were not up- or down-crossed by the observed change, the temporal variability over the data time period was insignificant.

Correlation analysis

Any possible linkage of the rainfall variability to the large scale ocean–atmosphere interactions was sought using correlation analysis (at both $\alpha = 5$ and 1%) under the null hypothesis H_0 'there is no correlation between the variability results of the rainfall and those of the climate indices'. The correlation analysis was carried out at both annual and seasonal time scales.

RESULTS AND DISCUSSION

Spatial differences in rainfall seasons

Figure 3 shows the long-term mean monthly rainfall. In Figure 3(a), it is seen that the rainfall over the equatorial region exhibits a bimodal pattern with the main wet
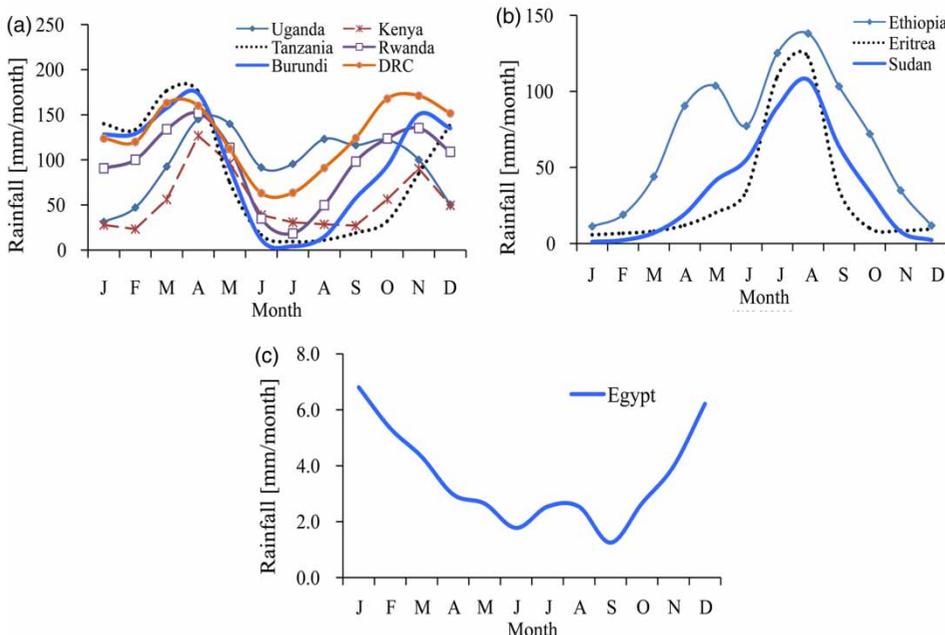
Figure 3 │ Pattern of mean long-term monthly rainfall.

season from March to May (MAM) and 'short rains' from October to December (OND). Two dry seasons exist as well; the main one is from June to September (JJAS) and the other from January to February (JF). Contrastingly, as shown in Figure 3(b), the main wet season of Sudan, Ethiopia, and Eritrea occurs in JJAS and 'short rains' are in MAM; there is one long dry season from October to February (ONDJF). For Egypt, the mean value of the rainfall in each month is far lower than those in Figure 3(a) and 3(b). However, it is noticeable that the wet seasons of Egypt cover MAM and ONDJF, and the dry season occurs in the period JJAS. For representativeness, these patterns of long-term mean monthly totals obtained using country-wide rainfall were crosschecked and found to agree with those presented by Onyutha & Willems (2015a) for data observed at some meteorological stations especially in Uganda, Tanzania, Burundi, Sudan, Ethiopia, Eritrea, and Egypt.

Spatial differences in the temporal rainfall variability

Figure 4 shows temporal variability of anomalies (results from the NAIM) for annual rainfall in the River Nile countries. In the 1920s, the equatorial region was characterized by the annual rainfall below the reference. This decrease was significant in Uganda, Tanzania, Rwanda, and Burundi; all these countries border one another. The period from the 1960s to early 1980s was characterized by rainfall being above average in Uganda, Rwanda, and Burundi. The increase in the 1960s was significant in Kenya, Rwanda, Burundi, and DRC. This finding is consistent with that of Kizza et al. (2009). Using station-based rainfall in the equatorial region, these authors concluded that the 1960s exhibited a significant upward jump in the rainfall of Lake Victoria Basin. Such a step change result could be supportive in understanding the impact of man's activities (such as deforestation, urbanization, agricultural practices, etc.) on the hydrology of the region. However, in the period between 2000 and 2012, the equatorial region was characterized by its rainfall above the reference. The periods with rainfall above or below the reference correspond to those also found by Mbungu et al. (2012) using station-based rainfall observed between 1920 and 2006.

In Sudan, rainfall was above the reference in the period 1920s up to around 1960 with a significant increase in the late 1950s. This was followed by a drastic and significant decrease in rainfall from the late 1960s to mid-1980s. In line with this decrease, Hulme (1992) found that the mean annual rainfall in the Sahel region (which spans across Central Sudan) for the 1970s and 1980s declined by 30%. Regarding changes in the wet season structure in Central Sudan, Hulme (1988) maintained that the said rainfall decrease from the 1960s led to much shorter rainy seasons in the 1970s and 1980s, mainly due to an earlier end. In Figure 4(j), it is evident that the periods with a significant increase and decrease in Egypt's rainfall were from the 1900s–1920 and 1930s–1960, respectively. In Eritrea, the periods with an increase (decrease) in rainfall were the 1930s, 1950s, and the late 1970s (1940s, 1960s, and mid-1990s); correspondingly for Ethiopia, the following were noted: the 1930s and 1970s (1940–1960s and 1980–2011). With data of shorter record length (from 1964 to 2004) than those used in this study, Taye & Willems (2011) reported that the upper Blue Nile Basin-wide total annual rainfall was above (below) the reference over the period 1960s to early 1980s (mid-1980s–2004). This is consistent with the results of this study as seen from Figure 4(h). Unlike in the equatorial region, the countries in the northern half of the River Nile over the period between 2000 and 2012 were characterized by their rainfall below the reference (Figure 4 (g) and 4(j)). Only results for the temporal variability of the annual rainfall are presented in Figure 4. Explanation of the spatio-temporal differences in the driving forces for the observed variability of the various seasons is also presented, as will now be discussed.

Spatio-temporal differences in the rainfall variability drivers

Figure 5 shows the temporal variability of the MAM rainfall in Ethiopia and those of the climate indices. It is shown that the anomalies of both annual rainfall and the AMO index follow each other fairly well. This means that the variation in MAM rainfall can be partly explained by that in AMO. For all the River Nile countries, correlation between anomaly patterns and those of climate indices as illustrated in Figure 5 are summarized in Table 3.

For the equatorial region (stations 1–6 in Table 1), the variability of the October–December (OND) (March-May (MAM)) rainfall was shown to have significant correlations
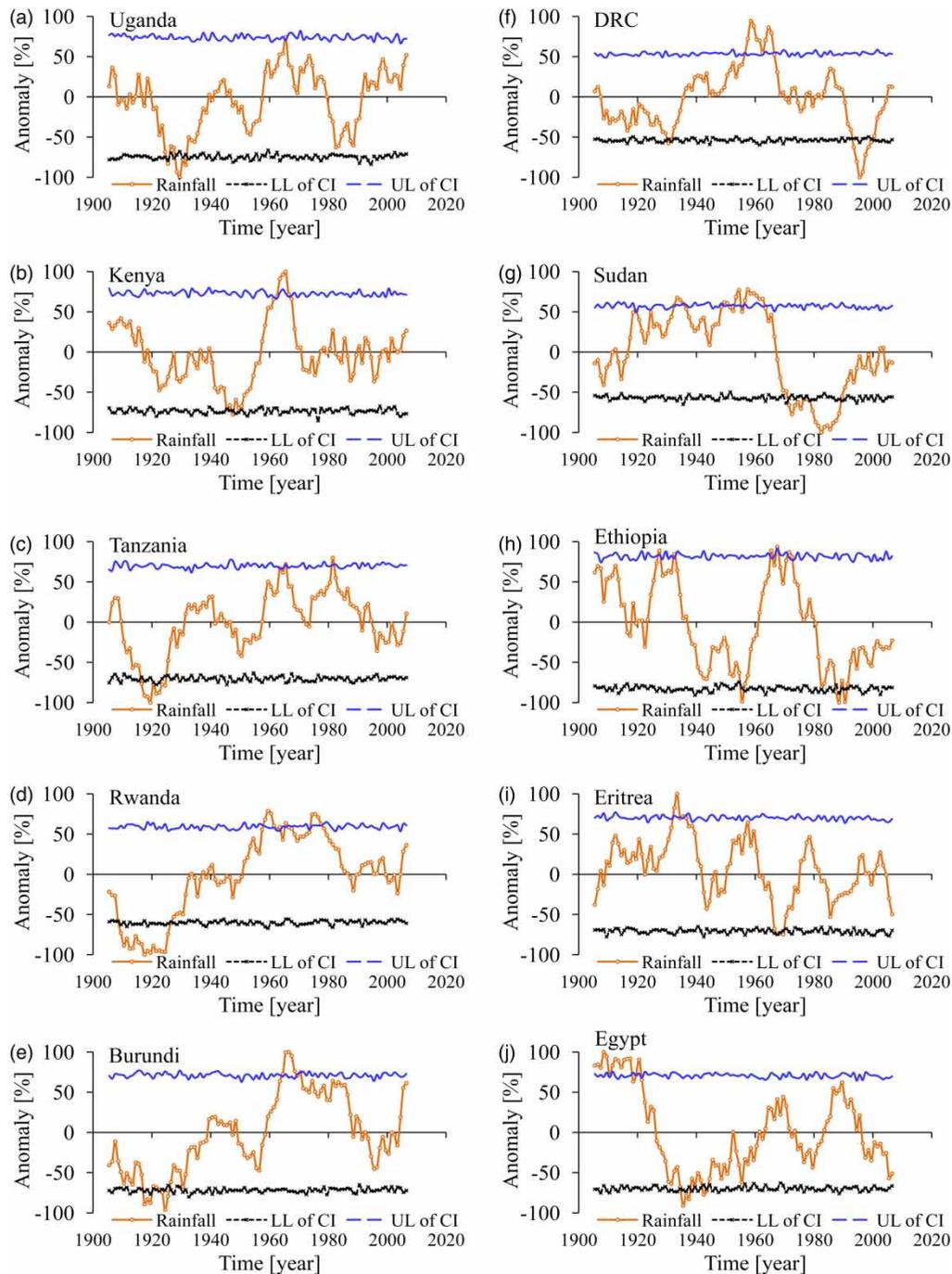
Figure 4 │ Results from the NAIM applied to the annual rainfall with time slice of 10 years over the period 1901–2011; UL (LL) is the upper (lower) limit of the 95% confidence interval (CI).

with Niño 4 and IOD (AMO). The variability in the JF rainfall was also noted to be influenced by those from the IOD and AMO. For most countries of the equatorial region, the variability in the annual rainfall was found to be significantly linked with influences from the Indian Ocean.

Influences from the Pacific Ocean in the form of PDO were not so conclusive for the annual (except the June to September (JJAS)) rainfall on a regional basis because the signs of the correlation coefficients were not consistent in most, if not all, of the countries. The linkage between the
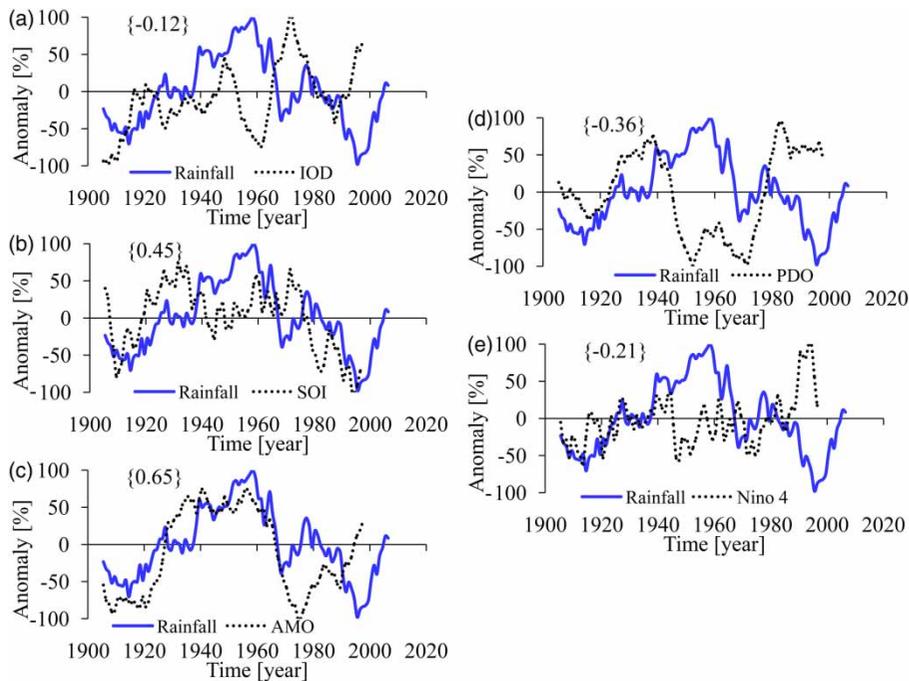
Figure 5 | Results from the NAIM applied to the March to May (MAM) rainfall and climate indices; the correlation coefficient between the two curves of each chart is put as label in {}.

rainfall of the equatorial region and the Indian Ocean was also found by Camberlin (1997), Awange et al. (2013), and Tierney et al. (2013). Significant correlation with Niño 4 is consistent with the results from a number of studies in which the influence of the ENSO on rainfall in the equatorial region was found; see, for example, Nicholson & Entekhabi (1986), Ropelewski & Halpert (1987), Ogallo (1989), Nicholson (1996), Nicholson & Kim (1997), Indeje et al. (2000), Philipps & McIntyre (2000), Schreck & Semazzi (2004), and Awange et al. (2013). It was shown that the signs of the correlation coefficients for the annual and the October–December (OND) rainfall were consistent. This means that drivers of variability in annual rainfall could be those that cause variations in the OND rainfall.

For the countries in the northern half of the River Nile, Table 3 shows that there was significant positive (negative) correlation between variability in the annual rainfall and SOI (Niño 4). Correspondingly for the June–September (JJAS) season, significant linkages were found with IOD (SOI). Significant correlation was found between SOI and the MAM rainfall of the countries in the northern part of the River Nile. These findings, again, agree with results from a number of previous studies. For instance, the influence of variability in the rainfall of the said region by the ENSO was found by

Osman & Shamseldin (2002) for Sudan; Grist & Nicholson (2001) for the Sahel belt; and Beltrando & Camberlin (1993), Seleshi & Demarée (1995), Seleshi & Zanke (2004), Segele & Lamb (2005), Korecha & Barnston (2007), Abtew et al. (2009), and Diro et al. (2010) for Ethiopia and Eritrea. The variability of annual and March–May (MAM) seasonal rainfall of Ethiopia was shown to have significant correlation with the occurrences in the Pacific and Atlantic Oceans. This is consistent with the results from a number of studies. Using station-based rainfall data, Taye & Willems (2012) and Moges et al. (2014) concluded that changes in the Pacific and Atlantic Oceans are the major natural causes of the variability in the rainfall over the Blue Nile Basin of Ethiopia. Jury (2010) also found that the rainfall variability of the northern and southern zones of Ethiopia are enhanced by the Atlantic and Pacific SST oscillation pattern in warm and cool phase, respectively. The variability in both annual and seasonal rainfall of Egypt was found to be significantly correlated with the influence from the Atlantic Ocean in terms of the AMO index.

Generally, it was shown that the magnitudes (and sometimes the signs) of the correlation between the NAIM results of rainfall with those of climate indices varied from one country to the next. This might have been due to randomness in the rainfall data or difference in microclimate

Table 3 | Correlation between anomaly in full series annual rainfall and annual climate indices

S no.	Country	Annual					MAM season				
		PDO	SOI	IOD	Niño 4	AMO	PDO	SOI	IOD	Niño 4	AMO
1	Uganda	**−0.50**	0.03	**0.27**	−0.10	−0.21	**−0.29**	0.05	−0.01	−0.04	**0.31**
2	Kenya	−0.10	−0.03	−0.16	0.10	**−0.27**	−0.23	−0.04	**−0.46**	−0.20	−0.24
3	Tanzania	0.14	**−0.34**	0.24	0.26	0.16	0.12	−0.01	−0.21	−0.03	**0.28**
4	Rwanda	**−0.29**	−0.15	**0.50**	0.14	0.23	−0.16	−0.14	**0.46**	0.17	**0.33**
5	Burundi	−0.19	**−0.27**	**0.59**	0.19	−0.06	−0.20	−0.08	0.20	−0.09	0.06
6	DRC	**−0.44**	0.10	−0.03	−0.20	**0.28**	**0.43**	0.25	0.12	0.12	−0.24
7	Sudan	**−0.35**	**0.48**	**−0.36**	**−0.28**	**0.69**	0.16	**0.39**	−0.01	0.05	**0.48**
8	Ethiopia	−0.21	**0.60**	−0.18	**−0.33**	**−0.35**	**−0.36**	**0.45**	−0.12	−0.21	**0.65**
9	Eritrea	0.26	0.23	**−0.46**	**−0.27**	**0.35**	**0.61**	**−0.43**	0.01	**0.30**	0.02
10	Egypt	−0.06	0.00	−0.22	−0.03	**−0.77**	−0.13	**−0.45**	0.08	−0.13	**−0.85**

S no.	Country	JJAS season					OND[a] (ONDJF[b]) season				
		PDO	SOI	IOD	Niño 4	AMO	PDO	SOI	IOD	Niño 4	AMO
1	Uganda	**−0.39**	**0.35**	−0.03	**−0.42**	0.14	−0.13	**−0.39**	**0.26**	**0.48**	**−0.39**
2	Kenya	−0.25	0.24	**0.27**	−0.14	−0.04	−0.10	−0.06	−0.02	0.24	−0.04
3	Tanzania	−0.22	**0.33**	−0.24	**−0.51**	0.00	0.10	**−0.43**	**0.52**	**0.58**	**−0.33**
4	Rwanda	−0.08	0.04	**0.38**	−0.02	−0.10	**−0.38**	−0.16	**0.36**	**0.28**	0.03
5	Burundi	0.06	0.04	0.19	−0.09	−0.20	−0.21	**−0.48**	**0.59**	**0.50**	0.00
6	DRC	**−0.49**	**0.60**	**−0.61**	**−0.60**	−0.17	**−0.45**	0.07	0.00	−0.02	−0.25
7	Sudan	**−0.58**	**0.42**	**−0.47**	**−0.35**	**0.51**	**−0.35**	0.24	−0.15	−0.13	**0.31**
8	Ethiopia	−0.17	0.12	0.12	−0.09	−0.24	−0.19	−0.03	−0.01	−0.03	0.15
9	Eritrea	−0.05	0.26	**−0.55**	**−0.47**	**0.30**	−0.15	−0.23	**0.55**	**0.43**	−0.18
10	Egypt	−0.10	**0.28**	**−0.61**	**−0.26**	**−0.30**	−0.02	0.10	**−0.34**	−0.02	**−0.59**

S no.	Country	JF season				
		PDO	SOI	IOD	Niño 4	AMO
1	Uganda	−0.18	0.18	−0.12	**−0.29**	−0.04
2	Kenya	−0.13	0.11	−0.14	−0.02	−0.13
3	Tanzania	−0.08	−0.05	0.26	0.23	**0.42**
4	Rwanda	−0.21	0.13	**0.29**	−0.15	**0.48**
5	Burundi	−0.05	−0.11	**0.46**	0.20	0.24
6	DRC	0.02	0.03	0.01	0.16	**−0.50**

The bold values are significant at the level of 1%. The critical value of the correlation coefficients at significant level of 5% is 0.20.
[a]For stations 1–6; [b]For stations 7–10.
PDO, Pacific Decadal Oscillation index; SOI, Southern Oscillation Index; IOD, Indian Ocean Dipole; AMO, Atlantic Multidecadal Oscillation; DRC, Democratic Republic of Congo; JF, January to February; MAM, March to May; JJAS, June to September; OND, October to December; ONDJF, October to February.

(micro-scale features). Importantly, this might have also been due to the connection of the rainfall variability with the influence of regional features (topography, water bodies, land cover, etc.) over atmospheric circulation. The

highlands which bind the Nile Basin to the east, from Eritrea to Kenya, restrict penetration of the easterlies from the Indian Ocean; an exception is the gap between the Ethiopian and Kenyan highlands (Camberlin 2009).

Furthermore, the highlands of the Rift Valley also block the moist, unstable westerly flow of the Congo air from reaching the coastal areas (especially of Ethiopia), leading to complex patterns of rainfall over the Ethiopian highlands (Nicholson 1996). According to Camberlin (2009), the East African Great Lakes, furthermore, tend to develop their circulation in the form of lake breezes which interact with slope circulation. The joint impact of these lake and upslope breezes is the afternoon convection. Quantifying these regional influences due to topography over atmospheric circulation could be important. This, although not undertaken in this study, can be carried out by regional numeric modeling while taking into account local topographical features alongside the three-dimensional lake dynamics to reproduce the region's climate.

CONCLUSION

This paper has assessed, using the NAIM, variability in the seasonal and annual rainfall across the River Nile countries. Possible driving influences of the rainfall variability were sought using a number of climate indices. The NAIM gave results which were consistent with those of previous studies. This showed its credibility for analysis of variability in hydrometeorological variables.

The period of high (low) rainfall was the 1960s to early 1980s (the 1920s) for the equatorial region of the Nile Basin, the 1930s and the 1970s (the 1940s–1960s and the 1980s–2011) for Ethiopia, the 1920s–1960 (the late 1960s to mid-1980s) for Sudan, the 1930s and late 1970s (the 1960s and mid-1990s) for Eritrea, and the 1900s–1920 (the 1930s–1960) for Egypt. The countries in the equatorial region (northern half) of the River Nile, over the period between 2000 and 2012 were characterized by their rainfall above (below) reference. Generally, the variability in the rainfall of the countries in the equatorial (northern) part of the River Nile was found to be correlated with those in the AMO and IOD (SOI and AMO) for the March–May season, and Niño 4 (Niño 4 and IOD) for the June–September season. Correspondingly for the variability of the annual rainfall, links to IOD (Niño 4 and AMO) were found.

Assessment of the possible influences of the large-scale ocean–atmosphere interactions on the variability of seasonal and annual rainfall volumes, as carried out in this study, makes it possible to get an insight into the considerable effect of the climate oscillations on water resources and agricultural management practices. When driving forces of the rainfall variability are known, it can be possible to separate natural variability or oscillations (of decadal cycles) from long-term trends (for instance due to global warming). This may be significantly useful especially in predicting upcoming periods of decrease or increase in the seasonal and annual rainfall volumes. Apart from the large ocean–atmosphere interactions, other possible driving forces of rainfall variability including water bodies, topography, transition in land cover and/or change, etc. should be investigated.

REFERENCES

Abtew, W., Melesse, A. M. & Dessalegne, T. 2009 El Niño Southern Oscillation link to the Blue Nile River basin hydrology. *Hydrol. Process.* **23**, 3653–3660.

Awange, J. L., Anyah, R., Agola, N., Forootan, E. & Omondi, P. 2013 Potential impacts of climate and environmental change on the stored water of Lake Victoria Basin and economic implications. *Water Resour. Res.* **49**, 8160–8173.

BADC 2014 *CRU year-by-year variation of selected climate variables by country.* http://badc.nerc.ac.uk/view/badc.nerc.ac.uk__ATOM__DE_56531370-2613-11e3-9fca-00163e251233 (retrieved 17 June 2014).

Beltrando, G. & Camberlin, P. 1993 Interannual variability of rainfall in the eastern horn of Africa and indicators of atmospheric circulation. *Int. J. Climatol.* **13**, 533–546.

Blackman, R. B. & Tukey, J. W. 1959 *The Measurement of Power Spectra.* Dover Publications, New York.

Bretherton, C. S., Smith, C. & Wallace, J. M. 1992 An intercomparison of methods for finding coupled patterns in climate data. *J. Climate* **5**, 541–560.

Buishand, T. A. 1982 Some methods for testing the homogeneity of rainfall records. *J. Hydrol.* **58**, 11–27.

Camberlin, P. 1997 Rainfall anomalies in the source region of the Nile and their connection with the Indian summer monsoon. *J. Climate* **10**, 1380–1392.

Camberlin, P. 2009 Nile Basin climates. In: *The Nile: Origin, Environments, Limnology and Human Use, Monographiae Biologicae vol. 89* (H. J. Dumont, ed.). Springer, Dordrecht, pp. 307–333.

Davidson, A. C. & Hinkley, D. V. 1997 *Bootstrap Methods and Their Application*. Cambridge University Press, Cambridge, UK, 582 pp.

Diro, G., Grimes, D. I. F. & Black, E. 2010 Teleconnections between Ethiopian summer rainfall and sea surface temperature: part I – observation and modelling. *Clim. Dyn.* **37**, 121–131.

Gichere, S. K., Olado, G., Anyona, D. N., Matano, A. S., Dida, G. O., Abuom, P. O., Amayi, A. J. & Ofulla, A. V. O. 2013 Effects of drought and floods on crop and animal losses and socio-economic status of households in the Lake Victoria Basin of Kenya. *J. Emerg. Trends Econ. Manage. Sci.* **4** (1), 31–41.

Grist, J. P. & Nicholson, S. E. 2001 A study of the dynamic forces influencing rainfall variability in the West Africa Sahel. *J. Climate* **14**, 1337–1359.

Harris, I., Jones, P. D., Osborn, T. J. & Lister, D. H. 2014 Updated high-resolution grids of monthly climatic observations – the CRU TS3.10 dataset. *Int. J. Climatol.* **34**, 623–642.

Horel, J. D. 1982 On the annual cycle of the tropical Pacific atmosphere and ocean. *Mon. Weather Rev.* **110**, 1863–1878.

Hulme, M. 1988 Changes in wet season structure in Central Sudan, 1900–86. In: *Recent Climatic Change* (S. Gregory, ed.). Belhaven Press, London, New York, pp. 179–192.

Hulme, M. 1992 Rainfall changes in Africa: 1931–1960 to 1961–1990. *Int. J. Climatol.* **12**, 685–699.

Hurst, H. E. 1951 Long-term storage capacity of reservoirs. *Trans. Am. Soc. Civ. Eng.* **116**, 770–799.

Indeje, M., Semazzi, H. F. M. & Ogallo, L. J. 2000 ENSO Signals in East African rainfall seasons. *Int. J. Climatol.* **20**, 19–46.

IWMI 2014 East Africa. http://eastafrica.iwmi.cgiar.org/ (retrieved 2 January 2014).

Jury, M. R. 2010 Ethiopian decadal climate variability. *Theor. Appl. Climatol.* **101**, 29–40.

Kibiiy, J., Kivuma, J., Karogo, P., Muturi, J. M., Dulo, S. O., Roushdy, M., Kimaro, T. A. & Akiiki, J. B. M. 2010 *Flood and Drought Forecasting and Early Warning*. Nile Basin Capacity Building Networks (NBCBN), Flood Management Research Cluster. Nile Basin Capacity Building Network (NBCBN-SEC) Office, Cairo, Egypt, 68 pp.

Kizza, M., Rodhe, A., Xu, C. -Y., Ntale, H. K. & Halldin, S. 2009 Temporal rainfall variability in the Lake Victoria Basin in East Africa during the twentieth century. *Theor. Appl. Climatol.* **98**, 119–135.

Kizza, M., Rodhe, A., Xu, C. -Y. & Ntale, H. K. 2011 Modelling catchment inflows into Lake Victoria: uncertainties in rainfall–runoff modelling for the Nzoia River. *Hydrol. Sci. J.* **56** (7), 1210–1226.

Kizza, M., Guerrero, J. -L., Rodhe, A., Xu, C. -Y. & Ntale, H. K. 2013 Modelling catchment inflows into Lake Victoria: regionalisation of the parameters of a conceptual water balance model. *Hydrol. Res.* **44** (5), 789–808.

Korecha, D. & Barnston, A. G. 2007 Predictability of June–September rainfall in Ethiopia. *Mon. Weather Rev.* **135**, 628–650.

Mantua, N. J., Hare, S. R., Zhang, Y., Wallace, J. M. & Francis, R. C. 1997 A Pacific interdecadal climate oscillation with impacts on salmon production. *Bull. Am. Meteorol. Soc.* **78**, 1069–1079.

Mbungu, W., Ntegeka, V., Kahimba, F. C., Taye, M. & Willems, P. 2012 Temporal and spatial variations in hydro-climatic extremes in the Lake Victoria basin. *Phys. Chem. Earth* **50–52**, 24–33.

McCartney, M. P. & Girma, M. M. 2012 Evaluating the downstream implications of planned water resource development in the Ethiopian portion of the Blue Nile River. *Water Int.* **37** (4), 362–379.

Melesse, A. M., Bekele, S. & McCornick, P. 2011 Introduction: hydrology of the Nile in the face of climate and land-use dynamics. In: *Nile River Basin: Hydrology, Climate and Water Use* (A. M. Melesse, ed.). Springer, Dordecht, pp. vii–xvii.

Moges, S. A., Taye, M. T., Willems, P. & Gebremichael, M. 2014 Exceptional pattern of extreme rainfall variability at urban centre of Addis Ababa, Ethiopia. *Urban Water J.* **11** (7), 596–604.

Nawaz, R., Bellerby, T., Sayed, M. & Elshamy, M. 2010 Blue Nile runoff sensitivity to climate change. *Open Hydrol. J.* **4**, 137–151.

Nicholson, S. E. 1996 A review of climate dynamics and climate variability in Eastern Africa. In: *The Limnology, Climatology and Paleoclimatology of the East African Lakes* (T. C. Johnson & E. O. Odada, eds). Gordon and Breach, Amsterdam, pp. 25–56.

Nicholson, S. E. & Entekhabi, D. 1986 The quasi-periodic behavior of rainfall variability in Africa and its relationship to Southern Oscillation. *J. Clim. Appl. Meteorol.* **26**, 561–578.

Nicholson, S. E. & Kim, J. 1997 The relationship of the El-Niño Southern Oscillation to African rainfall. *Int. J. Climatol.* **17**, 117–135.

Ntegeka, V. & Willems, P. 2008 Trends and multidecadal oscillations in rainfall extremes, based on a more than 100-year time series of 10 min rainfall intensities at Uccle, Belgium. *Water Resour. Res.* **44** (7), W07402.

Nyeko-Ogiramoi, P., Willems, P., Mutua, F. & Moges, S. A. 2012 An elusive search for regional flood frequency estimates in the River Nile basin. *Hydrol. Earth Syst. Sci.* **16**, 3149–3163.

Nyeko-Ogiramoi, P., Willems, P. & Ngirane-Katashaya, G. 2013 Trend and variability in observed hydrometeorological extremes in the Lake Victoria basin. *J. Hydrol.* **489**, 56–73.

Ogallo, L. J. 1989 The spatial and temporal patterns of the eastern Africa seasonal rainfall derived from principal component analysis. *Int. J. Climatol.* **9**, 145–167.

Onyutha, C. 2016 Identification of sub-trends from hydro-meteorological series. *Stoch. Environ. Res. Risk Assess.* **30** (1), 189–205. http://dx.doi.org/10.1007/s00477-015-1070-0.

Onyutha, C. & Willems, P. 2013 Uncertainties in flow-duration-frequency relationships of high and low flow extremes in Lake Victoria basin. *Water* **5** (4), 1561–1579.

Onyutha, C. & Willems, P. 2015a Spatial and temporal variability of rainfall in the Nile Basin. *Hydrol. Earth Syst. Sci.* **19**, 2227–2246.

Onyutha, C. & Willems, P. 2015b Uncertainty in calibrating generalised Pareto distribution to rainfall extremes in Lake Victoria basin. *Hydrol. Res.* **46** (3), 356–376. http://dx.doi.org/10.2166/nh.2014.052.

Onyutha, C. & Willems, P. 2015c Empirical statistical characterisation and regionalisation of amplitude-duration-frequency curves for extreme peak flows in the Lake Victoria basin. *Hydrol. Sci. J.* **60**, 997–1012. http://dx.doi.org/10.1080/02626667.2014.898846.

Osman, Y. Z. & Shamseldin, A. Y. 2002 Qualitative rainfall prediction models for central and Southern Sudan using El Niño-Southern Oscillation and Indian Ocean sea surface temperature indices. *Int. J. Climatol.* **22**, 1861–1878.

Philipps, J. & McIntyre, B. 2000 ENSO and interannual rainfall variability in Uganda: implications for agricultural management. *Int. J. Climatol.* **20**, 171–182.

Rayner, N. A., Parker, D. E., Horton, E. B., Folland, C. K., Alexander, L. V., Rowell, D. P., Kent, E. C. & Kaplan, A. 2003 Global analyses of sea surface temperature, sea ice, and night marine air temperature since the late nineteenth century. *J. Geophys. Res.* **108** (D14), 4407.

Ropelewski, C. F. & Halpert, M. S. 1987 Global and regional scale precipitation patterns associated with El Niño/Southern Oscillation. *Mon. Weather. Rev.* **115**, 1606–1626.

Ropelewski, C. F. & Jones, P. D. 1987 An extension of the Tahiti-Darwin Southern Oscillation Index. *Mon. Weather Rev.* **115**, 2161–2165.

Schreck, C. J. & Semazzi, F. H. M. 2004 Variability of the recent climate of Eastern Africa. *Int. J. Climatol.* **24**, 681–701.

Segele, Z. T. & Lamb, P. J. 2005 Characterization and variability of Kiremt rainy season over Ethiopia. *Meteorol. Atmos. Phys.* **89**, 153–180.

Seleshi, Y. & Demarée, G. R. 1995 Rainfall variability in the Ethiopian and Eritrean highlands and its links with the Southern Oscillation Index. *J. Biogeogr.* **22**, 945–952.

Seleshi, Y. & Zanke, U. 2004 Recent changes in rainfall and rainy days in Ethiopia. *Int. J. Climatol.* **24**, 973–983.

Semazzi, F. H. M. & Indeje, M. 1999 Inter-seasonal variability of ENSO rainfall signal over Africa. *J. Afr. Meteorol. Soc.* **4**, 81–94.

Sutcliffe, J. V., Ducgdale, G. & Milford, J. R. 1989 The Sudan floods of 1988. *Hydrol. Sci. J.* **34**, 355–365.

Taye, M. T. & Willems, P. 2011 Influence of climate variability on representative QDF predictions of the upper Blue Nile Basin. *J. Hydrol.* **411**, 355–365.

Taye, M. T. & Willems, P. 2012 Temporal variability of hydroclimatic extremes in the Blue Nile basin. *Water Resour. Res.* **48**, W03513.

Tierney, J. E., Smerdon, J. E., Anchukaitis, K. J. & Seager, R. 2013 Multidecadal variability in East African hydroclimate controlled by the Indian Ocean. *Nature* **493**, 389–392.

Trenberth, K. E. 1997 The definition of El Niño. *Bull. Am. Meteorol. Soc.* **78**, 2771–2777.

Trenberth, K. E. & Shea, D. J. 2006 Atlantic hurricanes and natural variability in 2005. *Geophys. Res. Lett.* **33** (12), L12704.

van Oldenborgh, G. J., te Raa, L. A., Dijkstra, H. A. & Philip, S. Y. 2009 Frequency- or amplitude-dependent effects of the Atlantic meridional overturning on the tropical Pacific Ocean. *Ocean Sci.* **5**, 293–301.

WMO 1966 Climatic change. Tech. Note No. 79, WMO, Geneva, Switzerland, 79 pp.